Limited Sampling Strategies for Therapeutic Drug Monitoring of Mycophenolate Mofetil Therapy in Patients With Autoimmune Disease

Brenda C. M. de Winter, PharmD, Irmgard Neumann, MD, PhD,† Reinier M. van Hest, PharmD, PhD,* Teun van Gelder, MD, PhD,* and Ron A. A. Mathot, PharmD, PhD**

Abstract: Mycophenolate mofetil (MMF) is increasingly used for the treatment of autoimmune diseases (AID). In renal transplant recipients, it has been demonstrated that adjustment of the MMF dose according to the area under the plasma concentration versus time curve (AUC) of mycophenolic acid (MPA), the active moiety of MMF, improves clinical outcome. The aim of this study was to develop a maximum a posteriori Bayesian estimator (MAP-BE) to estimate MPA $AUC_{0–12}$ in patients with AID using a limited number of samples. The predictive performance of the MAP-BE was compared with a multiple linear regression method. Full MPA concentration versus time curves were available from 38 patients with AID treated with MMF. Nonlinear mixed-effect modeling was used to develop a population pharmacokinetic model. Patients were divided in an index and a validation data set. The pharmacokinetic model derived from the index data set was used to develop several MAP-BEs. The Bayesian estimators were used to predict $AUC_{0–12}$ in the validation data set on the basis of a limited number of blood samples. The bias and precision of these predictions were compared with those of limited sampling strategies developed with multiple linear regression. The absorption of MPA was described with 2 first-order processes with a short and a long lag time and a subsequent first-order elimination. The 2-compartment model accounted for the enterohepatic recirculation of MPA as well. Using 1–4 samples, MPA $AUC_{0–12}$ was adequately estimated by the MAP-BE. Bias (−5.5%) was not significantly different from zero, and precision was below 27%. The predictive performance of the multiple linear regression method was comparable. In conclusion, MAP-BEs were developed for the estimation of MPA $AUC_{0–12}$ in patients with AID. The predictive performance was good and comparable to those of the multiple linear regression method. Due to its flexibility with respect to sample times, the MAP-BE may be preferred over the multiple linear regression method.

Key Words: mycophenolate mofetil, mycophenolic acid, therapeutic drug monitoring, autoimmune disease, limited sampling strategy

(*Ther Drug Monit* 2009;31:382–390)

INTRODUCTION

Mycophenolate mofetil (MMF) is now the most prescribed drug for renal transplant recipients.[1] After oral administration, the prodrug MMF is rapidly hydrolyzed to the active agent mycophenolic acid (MPA). The majority of MPA is metabolized to the inactive 7-O-mycophenolic acid glucuronide (MPAG), which undergoes enterohepatic recirculation (EHC). MPA inhibits the immune system due to a selective reversible inhibition of inosine monophosphate dehydrogenase.[2] Although introduced as a fixed-dose drug, debate has emerged with respect to the potential contribution of monitoring MPA plasma concentrations as a basis for MMF dose adjustment [therapeutic drug monitoring (TDM)].[3,4] The between-patient variability in MPA pharmacokinetics[5] and the observation that the risk for acute rejection increases with lower MPA plasma concentrations suggest that a strategy of TDM for MMF therapy could improve outcome.[6,7] Evidence for the added value of TDM of MPA comes from a recent randomized study in adult renal transplant recipients, where a significantly lower incidence of biopsy-proven acute rejection was found in the TDM-based dosing group compared with a fixed-dose group.[8]

The most reliable assessment of MPA exposure is obtained through the repetitive measurement of 12-hour MPA area under the concentration–time curves ($AUC_{0–12}$). Unfortunately, routine application of the full MPA $AUC_{0–12}$ regimen, consisting of 8–10 samples drawn over a 12-hour time interval, is impractical from a clinical point of view. Predose assessment of MPA is a commonly used alternative to MPA $AUC_{0–12}$. However, correlations between predose concentrations and MPA $AUC_{0–12}$ are relatively weak ($r^2 = 0.4–0.5$),[9] and there is greater within-patient variability for predose concentrations than for $AUC_{0–12}$. Abbreviated AUC strategies have been proposed to represent the best of both worlds, yielding greater accuracy than predose measurements, although being less cumbersome than a 12-hour sampling strategy. For MPA, limited sampling strategies (LSSs) using a predose sample and

Received for publication November 4, 2008; accepted February 23, 2009.
From the *Department of Hospital Pharmacy, Erasmus University Medical Center, Rotterdam, The Netherlands; and †Department of Nephrology, Wilhelminenspital, Vienna, Austria.
Correspondence: Brenda C. M. de Winter, PharmD, Department of Hospital Pharmacy, Erasmus University Medical Center, Room L-056, PO Box 2040, 3000 CA Rotterdam, The Netherlands (e-mail: b.dewinter@erasmusmc.nl).

2 postdose samples have shown good agreement between the estimated and measured AUC, with correlation coefficients (r^2) ranging from 0.84 to 0.95.[9–11]

Following anecdotal reports describing benefits of MMF in patients with systemic lupus erythematosus (SLE) and lupus nephritis, small studies and finally large, randomized, controlled trials have established the use of MMF in these patients, particularly those with lupus nephritis.[12] MMF use in other autoimmune disease (AID), like antineutrophil cytoplasmic antibody–associated systemic vasculitis, has only been evaluated in smaller studies and in very few randomized controlled trials.[13] Many studies currently are ongoing with this immunosuppressive agent.[14–18] The publication of the Phase III Aspreva Lupus Management Study,[19] comparing induction therapy with MMF or cyclophosphamide in combination with corticosteroids for 24 weeks for lupus nephritis, and maintenance treatment with MMF or azathioprine thereafter is expected in 2009.

Interindividual variability of MMF pharmacokinetic parameters in patients with AID was found to be as high as in renal transplant patients.[20] Whereas in renal transplant patients, treatment regimens often consist of 3 or 4 immunosuppressive drugs, AIDs are typically treated with 1 or 2 drugs concomitantly. This would imply that the success of the treatment would be even more dependent on the MPA concentrations reached, and thus, TDM in patients with AID may be a valuable tool to optimize individual immunosuppressive therapy.[21] Recently, a correlation is seen between MPA through levels and recurrence of active disease in patients with AID.[22] To facilitate prospective trials, we decided to develop and validate a maximum a posteriori Bayesian estimator (MAP-BE) for MMF treatment in patients with AID and compare the predictive performance of this MAP-BE with an LSS based on linear regression for estimating MPA exposure.

METHODS

Patients

Concentration–time samples from 38 patients (20 males and 18 females; age (mean ± SD) 52.4 ± 18.3 years) with AID treated with MMF who participated in a pharmacokinetic study were analyzed retrospectively. This study was based on a set of patients of whom the relationship between MPA concentrations and clinical outcome is already published.[22] This article describes the development of LSSs for the estimation of MPA $AUC_{0–12}$ in patients with AID, using the same data set. See Neumann et al[22] for a detailed description of the methods of this pharmacokinetic study. The clinical study was institutional review board approved. For the post hoc analysis of the data as described in this article, no additional institutional review board approval was requested as all data were anonimized. Briefly, 26 patients with antineutrophil cytoplasmic antibody–associated systemic vasculitis and 12 patients suffering from SLE were enrolled in the pharmacokinetic study. The patients received MMF (1 g twice daily) for at least 10 weeks before the study. More than half of the patients received a low dose of steroids (2.5–7.5 mg prednisolone) as comedication. Three patients (8%) used ciclosporin as a concomitant immunosuppressive drug. After a 12-hour overnight fast, a 1-g dose of MMF was administered orally. Blood samples were collected before drug intake and then 0.33, 0.67, 1, 1.5, 2, 3, 4, 6, 8, 12, 14, and 24 hours thereafter. During the 24-hour collection period, no additional MMF dose was given. Concentrations of MPA in plasma were determined using enzyme multiplied immunoassay technique assay (EMIT MPA Assay System; Dade Behring, San Jose, CA). The main characteristics of the patients are listed in Table 1.

Pharmacokinetic Modeling

Basic Model

All data were analyzed simultaneously using the nonlinear mixed-effects modeling software program (NONMEM Version VI, level 1.0; GloboMax LLC, Ellicott City, MD). Because NONMEM estimated pharmacokinetic parameters for MPA, MMF doses were converted to the equivalent MPA content by multiplying the MMF dose by 0.739. Data were logarithmically transformed, and the first-order estimation method was used throughout the entire model-building process because the first-order conditional estimate method did not minimize successfully.

In the first step of the population analysis, a compartmental pharmacokinetic model was developed. Several structural models were tested. Models with 1 or 2 compartments were evaluated, as well as models with and without lag time.

TABLE 1. Patient Characteristics

	Index Data Set (n = 19)	Validation Data Set (n = 19)	*P*
Sex (m/f)	11/8	7/12	0.53
Age (yrs)	50.0 ± 8.5 (20–82)	54.5 ± 7.7 (25–79)	0.91
Weight (kg)	73.4 ± 6.8 (45–111)	71.5 ± 7.7 (48–106)	0.51
Serum albumin (g/L)	43.3 ± 1.7 (34.0–49.8)	45.6 ± 2.3 (35.9–54.6)	0.30
Creatinine clearance (mL/min)	62.3 ± 12.5 (32.8–108)	70.5 ± 14.7 (16–136)	0.61
Proteinuria (g/24 h)	0.69 ± 0.35 (0–2.5)	0.59 ± 0.4 (0–3.7)	0.61
Hemoglobin (g/dL)	12.5 ± 0.5 (10–14.7)	12.3 ± 0.7 (8.9–14.1)	0.22
Primary disease	13 AASVs	13 AASVs	—
	6 SLEs	6 SLEs	—

For the index and validation groups, the patient characteristics are expressed as mean ± 95% confidence interval (range).
AASV, antineutrophil cytoplasmic antibody–associated vasculitis.

Furthermore, it was evaluated whether absorption was best described as a zero-order or FO process with single- or double-peak absorption profiles. Finally, several methods were evaluated to describe the EHC peak.[23,24] Pharmacokinetic parameters were estimated in terms of central and peripheral volume of distribution (V), clearance (CL), and intercompartmental clearance (Q). Because bioavailability (F) could not be quantified, V, CL, and Q values correspond to the ratios V/F, CL/F, and Q/F, respectively. Interpatient variability (IPV) for all pharmacokinetic parameters was modeled using an exponential (equation 1a) or additive (equation 1b) error model.

$$\mathrm{CL}_i = \theta_{\mathrm{pop}} \exp(\eta_i) \quad (1a)$$

$$\mathrm{CL}_i = \theta_{\mathrm{pop}} + (\eta_i), \quad (1b)$$

where CL_i represents the MPA clearance of the ith individual, θ_{pop} represents the population value for MPA clearance, and η represents the interindividual random effect with mean 0 and variance ω^2. The covariance between values for IPV was estimated using a variance–covariance matrix. Residual variability between observed (C_{obs}) and predicted (C_{pred}) MPA plasma concentrations was described using an additional error model for logarithmic transformed data (equation 2).

$$\ln C_{\mathrm{obs}} = \ln C_{\mathrm{pred}} + \varepsilon_i, \quad (2)$$

where ε represents the residual random error with mean 0 and variance σ^2.

The population model was built stepwise. A specific assumption was tested at each step. The main decision criterion was the likelihood ratio test. In NONMEM modeling, the minimum value of objective function (OFV) can be used as a criterion for model selection. If the difference in OFV between 2 nested models is larger than the critical value from a χ^2 distribution with degrees of freedom equal to the difference in the number of estimated parameters, the models are significantly different from each other. A decrease in the OFV >10.83 shows a significant improvement of a nested model with 1 *df* of $P < 0.001$. Model adequacy was further evaluated by using various residual plots ("goodness-of-fit" plots) and values of random effects variances. To analyze the graphical goodness of fit, extensive plotting was available through the use of Xpose,[25] a purpose built set of subroutines in S-plus (version 6.1; Insightful Corp, Seattle, WA).

Covariate Model

To explain IPV, relationships were investigated between pharmacokinetic parameters and patient characteristics. Covariates tested were patient age, sex, weight, AID, concurrent use of ciclosporin, serum creatinine concentration, creatinine clearance (CrCL), proteinuria, hemoglobin, serum albumin concentration, lymphocyte, and leukocyte count. First, all potential covariates were added separately to the basic model for univariate analysis. Continuous covariates were modeled exponentially (equation 3).

$$\mathrm{CL}_{\mathrm{ij}} = \theta_{\mathrm{pop}}(\mathrm{CrCL}/66)^{\theta_{\mathrm{CrCL}}}, \quad (3)$$

in which θ_{pop} is the MPA CL in individuals with the median CrCL of the population (66 mL/min) and θ_{CrCL} is an exponent determining the shape of the relationship.

Categorical variables were modeled proportionally (equation 4).

$$\mathrm{CL}_{\mathrm{ij}} = \theta_{\mathrm{pop}}\theta^{\mathrm{CsA}}, \quad (4)$$

in which θ_{pop} is the MPA CL in individuals without ciclosporin (CsA = 0) and θ_{CsA} is the fractional change of CL due to concurrent use of ciclosporin. Whether a variable had a significant effect was determined with the likelihood ratio test. When inclusion of a covariate causes a decrease in OFV >3.84 ($P < 0.05$), the covariate was considered to be statistically significant.

Second, a multivariate analysis with backward elimination was done to obtain the final model. All covariates selected during the first stage were included in an intermediate model. Covariates were excluded separately from the intermediate model. If the elimination of a covariate caused an increase in OFV >10.8 ($P < 0.001$), then the covariate remained in the model.

Model Validation

As an internal validation method, a bootstrap resampling method[26] was applied, using the Wings for NONMEM software (Dr. N. Holford, version 612, March 2007, Auckland, New Zealand). Two hundred bootstrap data sets were generated by sampling randomly from the original data set with replacement. Parameters were estimated for each of the replicate data sets using the final model. The validity of the model was evaluated by comparing the median values and 95 percentiles of the bootstrap replicates with the estimates of the original data set.

The final model was further validated by the application of a visual predictive check.[27] One hundred data sets were simulated from the original data set using the final model. Per time point, the median simulated concentrations plus 95-percentile intervals were compared graphically with the observed MPA concentrations.

Limited Sampling Strategies

Design of MAP-BEs

The patient data set was split into 2 data sets: an index data set (n = 19) and a validation data set (n = 19). The index data set was used to obtain population parameter values of the final model. MAP-BEs were developed using the post hoc option of NONMEM. The best LSSs were selected on the basis of a combination of 1, 2, or 3 sampling times within 4 hours post dose. The individual parameters and AUC_{0-12} of the patients were estimated using the population model. Subsequently, the predictive performance of the developed MAP-BEs was evaluated with the validation data set by calculating bias or mean prediction error (equation 5) and precision or root mean squared prediction error (equation 6).

$$\mathrm{MPE} = \frac{\sum_{i=1}^{\mathrm{N}}(\mathrm{pe}_i)}{\mathrm{N}} \quad (5)$$

$$\mathrm{RMSE} = \sqrt{\frac{\sum_{i=1}^{\mathrm{N}}(\mathrm{pe}_i^2)}{\mathrm{N}}}, \quad (6)$$

where N represents the number of pairs of estimated and measured AUC, and pe_i is the difference between the estimated

and the measured AUC. Reference $AUC_{0–12}$ values were calculated using the linear trapezoidal rule and all available data concentrations. To assess the agreement between the calculated $AUC_{0–12}$ and the reference $AUC_{0–12}$, the r^2 was calculated.

LSSs Developed With Multiple Linear Regression

A second method, multiple linear regression, was used to develop an LSS as well. The index data set was used to develop the LSSs. MPA concentrations at each sampling time point were correlated with the reference $AUC_{0–12}$ using linear regression analysis. Those sampling time points that showed the best correlation were combined to create LSSs. The correlation was calculated in a multiple stepwise linear regression analysis, with the reference $AUC_{0–12}$ as independent variable and the MPA concentrations at the different sample time points as explanatory variables. The validation data set was used to determine bias, precision, and r^2 of the LSSs. These results were compared with the MAP-BEs.

RESULTS

Patients

The data set contained 492 MPA plasma concentrations obtained from 38 patients with AID. Each patient participated in 1 pharmacokinetic assessment of a 24-hour AUC. Figure 1 shows the observed MPA plasma concentration–time profiles for all patients. In some patients, a second and third peak was seen at approximately 6 and 10 hours after administration. Mean $AUC_{0–12}$ was 66.0 $mg \cdot h \cdot L^{-1}$, with a range between 27.6 and 129.4 $mg \cdot h \cdot L^{-1}$.

Pharmacokinetic Modeling

The concentration–time data of all patients were fitted simultaneously to several pharmacokinetic models. Figure 2 shows the final basic model. A 2-compartment model with a central (V_C) and a peripheral volume of distribution (V_P) and "first-order" elimination adequately described the data. To describe the absorption phase, a double-peak model with a short lag time ($T_{LAG,\ short}$) and a longer lag time ($T_{LAG,\ long}$) followed by "first-order" absorption was used. The fraction of the dose transported through the short (P) and long absorption compartments ($1-P$) was estimated. The EHC was modeled with an extra gallbladder compartment, which was filled continuously from the central compartment with rate k_{46}. Emptying of the gallbladder into the gastrointestinal compartment occurred at 2 time points (T_{GB1} and T_{GB2}) with rate k_{63} and duration D_{GB}, followed by reabsorption of MPA into the central compartment. Because insufficient data were collected around the EHC process, several parameters need to be fixed based on prior information to make the model numerically identifiable. The part of MPA clearance that was recirculated into the gallbladder (EHCP), calculated with equation 7, was fixed at 37%.

$$\mathrm{EHCP} = \frac{k_{46}}{k_{46} + \mathrm{CL}/V_C} \times 100\%. \quad (7)$$

The best values for the parameters T_{GB1}, T_{GB2}, D_{GB}, and k_{63} were determined after fixing these parameters at several values. The best values for these parameters resulted in a bolus (D_{GB} = 0.1 hours) gallbladder emptying at 6 and 10 hours after MMF administration. The optimal rate of emptying was 1 per hour.

Introduction of IPV for k_a, V_C, and CL as an exponential error model significantly improved the fit of the model; corresponding values were 186%, 54%, and 41%. Introduction of IPV of $T_{LAG,\ long}$, T_{GB1}, and EHCP further improved the fit of the model. IPV for these parameters however had to be fixed at certain values. IPV of EHCP was described exponentially and fixed at a value of 35%, which limited the EHCP of 95% of the patients between 10% and 61%.[28,29] For $T_{LAG,\ long}$, IPV was fixed at 32% with an exponential error model. With this restriction, it was possible to discriminate between delayed absorption ($T_{LAG} < 1$ hour) and EHC. The latter occurred usually after at least 4 hours. The longest individual absorption lag time estimated was 0.83 hours. The first EHC peak in the individual pharmacokinetic profiles varied between approximately 4 and 8 hours after administration. To get 95% of all first EHC peaks within this range, the IPV of T_{GB1} was fixed at an additive error value of 2 hours, resulting in a range of 2.3–7.9 hours. The second EHC peak (T_{GB2}) was fixed at a value of 4 hours after T_{GB1}. Typical population estimates for the pharmacokinetic parameters for this basic model are summarized in Table 2.

The screening of the relationship between patient factors and pharmacokinetic parameters produced an intermediate model with the following correlations: age, creatinine concentration, and leukocyte count for K_a; age, creatinine concentration, and CrCL for CL; and sex, kind of disease, creatinine concentration, and CrCL for EHCP ($P < 0.05$). During the backward elimination, only CrCL for CL resulted in a significant increase in OFV when excluded from the intermediate model (ΔOFV = 14.1, $P < 0.001$). Figure 3 shows the correlation between CrCL and MPA CL. The inclusion of this covariate in the final model partly explained IPV (Table 2). The estimate for IPV for CL decreased from 40.5% to 34.0%. Figure 4 illustrates the goodness-of-fit plots of the final model. The scatter plots of predicted and individually predicted versus

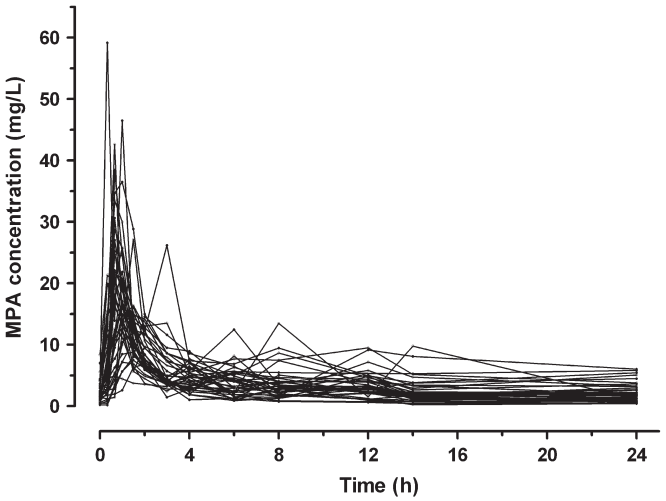

FIGURE 1. MPA concentration—time profiles. Pharmacokinetic curves obtained in 38 patients with AIDs receiving 1 g MMF.

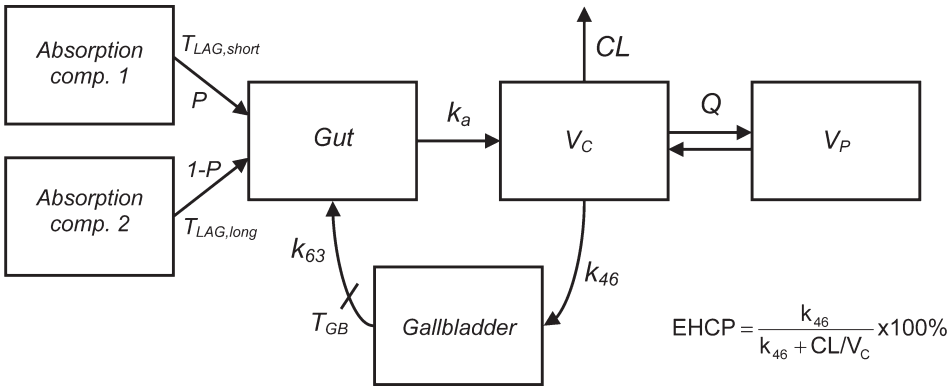

FIGURE 2. Population pharmacokinetic model. Model used to describe MPA concentration–time profiles in patients with AIDs. *P*, part of dose transported through the absorption compartment with short T_{LAG}; $T_{LAG,\ short}$, short lag time; $T_{LAG,\ long}$, long lag time; k_a, rate of absorption; V_C, volume of distribution of the central compartment; CL, clearance; V_P, volume of distribution of the peripheral compartment; *Q*, intercompartmental clearance; k_{46}, filling rate of gallbladder; T_{GB}, time of gallbladder compartment opening; EHCP, part of MPA recycled in the body; and k_{63}, rate of gallbladder emptying.

observed concentrations show no structural bias, except for a small underprediction of the maximum MPA concentration. The weighted residuals were homogeneously distributed over the sampling time period.

The results of 200 bootstrap replicates are given in Table 2. The mean estimates resulting from the bootstrap procedure are very similar to the population estimates of the final model. This demonstrated that the estimates for the fixed and random effects in the final model are accurate and that the model is stable.[26] The visual predictive check (Fig. 5) revealed a good agreement between the simulated and observed concentrations at all sampling time points. However, there seemed to be a small underprediction of the maximum MPA concentration at approximately 1 hour after MMF administration.

TABLE 2. Parameter Estimates of the Pharmacokinetic Models

	Basic Model		Final Model		Bootstrap		Index Data Set	
Parameter	**Value**	**OFV = −116.9 CV (%)**	**Value**	**OFV = −130.8 CV (%)**	**Mean**	**CV (%)**	**Value**	**CV (%)**
F_{fast}	0.718	10	0.713	9	0.704	20	0.675	13
$T_{LAG,\ short}$(h)	0.288	5	0.287	5	0.278	14	0.304	3
$T_{LAG,\ long}$(h)	0.643	3	0.645	3	0.624	17	0.663	1
k_a(h^{-1})	6.19	25	6.2	22	8.87	123	8.87	36
V_C(L)	51.8	11	52.4	17	50.7	16	50.0	16
CL (L/h)	7.92	8	8.27	5	7.34	19	8.61	8
V_P(L)	279	41	262	5	440	79	205	39
Q(L/h)	15.9	16	16.2	22	17.8	15	18.1	24
T_{GB1}(h)*	6	—	6	—	6	—	6	—
T_{GB2}(h)*	T_{GB1}+ 4	—	T_{GB1}+ 4	—	T_{GB1}+ 4	—	T_{GB1}+ 4	—
D_{GB}(h)*	0.1	—	0.1	—	0.1	—	0.1	—
EHCP*	0.37	—	0.37	—	0.37	—	0.37	—
K_{63}(h^{-1})*	1	—	1	—	1	—	1	—
ERR	0.415	6	0.414	6	0.503	37	0.409	9
CrCL on CL	—	—	0.42	26	0.408	7	0.454	35
IPV								
$T_{LAG,\ long}$(%)*	32	—	32	—	32	—	32	—
k_a(%)	186	32	182	40	141	98	200	55
V_C(%)	53.8	47	53	48	78	33	72	64
CL (%)	40.5	31	34	41	64.3	49	34	51
T_{GB1}(%)*†	200	—	200	—	200	—	200	—
EHCP (%)*	35	—	35	—	35	—	35	—

Estimations and their coefficient of variation for the pharmacokinetic parameters of the basic model, the final model, the index data set with the final model, and the bootstrap procedure are described in this table.

OFV, value of objective function; F_{fast}, part of dose ending up in the fast absorption compartment; $T_{LAG,\ short}$, lag time short absorption; $T_{LAG,\ long}$, lag time long absorption; k_a, rate of absorption; V_C, volume of distribution of the central compartment; CL, clearance; V_P, volume of distribution of the peripheral compartment; *Q*, intercompartmental clearance; T_{GBn}, time of nth opening gallbladder compartment; D_{GB}, duration of gallbladder opening; EHCP, part of MPA recycled in the body; k_{63}, rate of gallbladder emptying; ERR, residual random error; CrCL, creatinin clearance; CV, coefficient of variation.

*The parameter is fixed at this value.

†Additional variability.

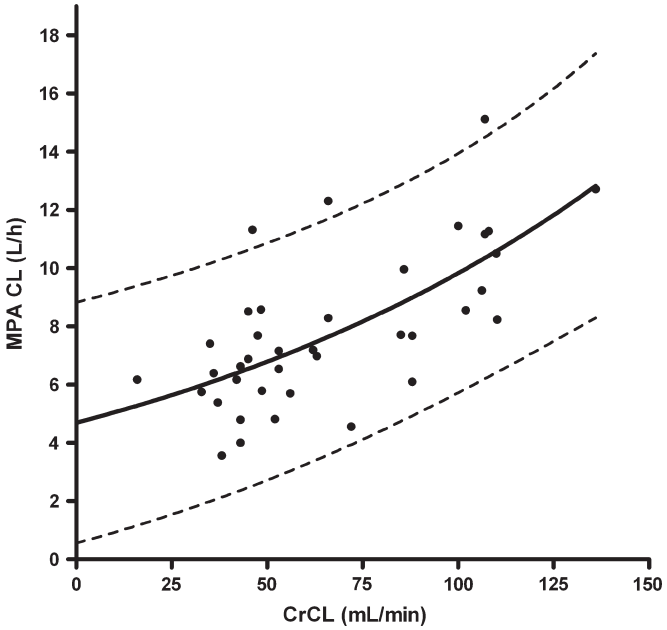

FIGURE 3. Correlation between creatinine clearance (CrCL) and MPA clearance (CL). Plot of the mean (solid line) influence of CrCL on MPA clearance and the 95% confidence interval of the predicted correlation (dotted lines).

Limited Sampling Strategies

The parameters of the final model were estimated again in the index data set, which produced comparable results (Table 2). The patient characteristics of the index and validation data sets were similar (Table 1). The population pharmacokinetic parameters obtained in the index group were used to develop MAP-BE to predict MPA $AUC_{0–12}$ on the basis of a limited number of samples. On the basis of predictive performance (bias and precision), the following sampling times between 0 and 4 hours post dose were selected for the optimal sampling schedules: 1 sample: 0 hour; 2 samples: 0 + 1 hour; 3 samples: 0 + 1 + 3 hours (Table 3). The developed MAP-BEs adequately estimated $AUC_{0–12}$ in the validation data set. When compared with $AUC_{0–12}$ assessed by the trapezoidal rule, bias was not significantly different from zero and precision was below 27%. An extra sample at 6 hours post dose was included in the LSS to provide more information about the extent of EHC. This extra sample improved the precision of the LSS from 23.0% to 18.9% (Table 3). The predictive performance for an individual patient is illustrated in Figure 6.

In the second LSS, multiple linear regression was used to select MPA plasma concentration sampling times to predict $AUC_{0–12}$. In the index data set, MPA concentrations at each sample time point until 4 hours after oral intake of MMF were correlated with the MPA $AUC_{0–12}$ as assessed by the trapezoidal rule. The correlation was best for the predose sample (r^2 = 0.68). The multiple stepwise regression analysis revealed that the best prediction of the measured $AUC_{0–12}$ was derived by the combination of the time points $t = 0 + 0.67$ hours post dose for a 2-sample LSS and $t = 0 + 1 + 3$ hours post dose for a 3-sample LSS (Table 3). Inclusion of the fourth sample (t = 6 hours) improved the predictive performance of the LSS. To test the agreement between the measured MPA $AUC_{0–12}$ and the predicted $AUC_{0–12}$, the developed LSSs were applied to the validation data set. The validation of the strategies yielded a precision below 27% and a bias not significantly different from zero.

DISCUSSION

In this study, a population pharmacokinetic model was developed for MPA in patients with AID (Fig. 2). In the model, the MPA concentration–time profiles were described by using a double-peak absorption model, a central and peripheral compartment and a gallbladder compartment for EHC. LSSs were developed on the basis of 1–3 samples during the first 4 hours after ingestion using MAP-BE and multiple linear regression. Both methods gave similar bias and precision. By increasing the number of sample times, the precision of the predicted $AUC_{0–12}$ increased. Sampling at 0, 1, and 3 hours after oral MMF administration resulted in the best predictive performance for both methods (Table 3). We would like to

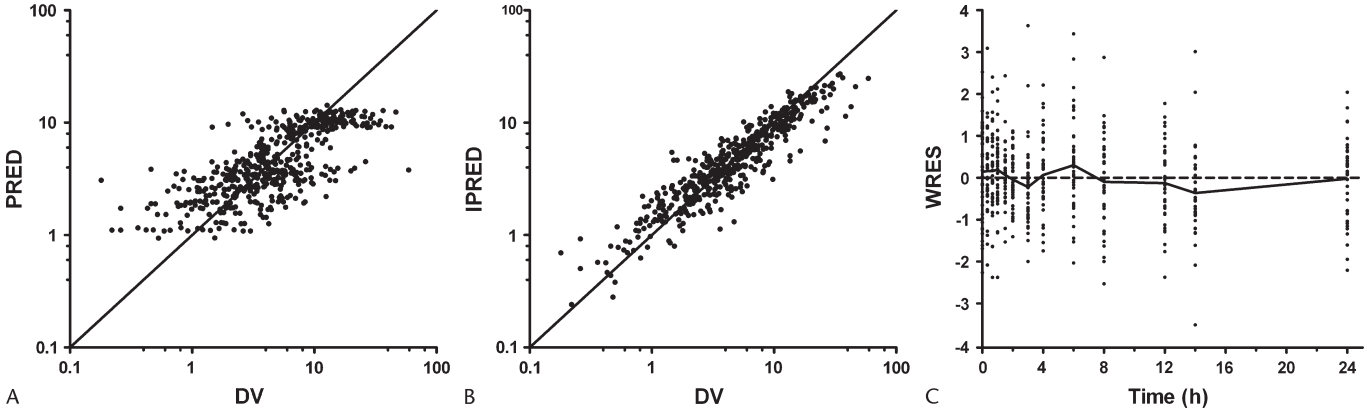

FIGURE 4. Goodness-of-fit plots of the final model. Plots of observed MPA concentration (DV) versus model predicted (PRED) (A) and Bayesian predicted (IPRED) (B) and weighted residuals (WRES) versus time (C). The solid line in (A) and (B) is the line of identity. The solid line in (C) is the average of the WRES.

TABLE 3. Predictive Performance of the LSSs in the Validation Data Set

Sampling Times LSS	Algorithm	Validation Data Set		
		MPE (%)	RMSE (%)	r^2
MAP-BE $t = 0$	—	−5.3 (−18.3, 7.7)	26.8 (13.1, 35.6)	0.38
MAP-BE $t = 0 + 1$	—	−5.6 (−17.6, 6.4)	24.9 (11.9, 32.4)	0.46
MAP-BE $t = 0 + 1 + 3$	—	−5.5 (−16.6, 5.6)	23.0 (12.6, 30.0)	0.53
MAP-BE $t = 0 + 1 + 3 + 6$	—	−5.5 (−14.4, 3.5)	18.9 (11.3, 24.2)	0.66
MLR $t = 0$	$AUC = 38.3 + 11.7 \times C_0$	3.4 (−9.8, 16.6)	26.8 (1.9, 37.9)	0.48
MLR $t = 0 + 0.67$	$AUC = 30.8 + 10.1 \times C_0 + 0.7 \times C_{0.67}$	4.8 (−7.4, 17.0)	25.1 (11.5, 33.5)	0.53
MLR $t = 0 + 1 + 3$	$AUC = 17.5 + 7.1 \times C_0 + 1.0 \times C_1 + 2.6 \times C_3$	0.8 (−10.4, 12.0)	22.6 (13.5, 29.0)	0.61
MLR $t = 0 + 1 + 3 + 6$	$AUC = 12.3 + 4.7 \times C_0 + 1.2 \times C_1 + 2.7 \times C_3 + 1.8 \times C_6$	−0.4 (−9.0, 8.1)	17.3 (9.0, 22.7)	0.70

Bias (MPE) and precision (RMSE) are represented as means and 95% confidence intervals.
MPE, mean prediction error; MLR, multilinear regression; RMSE, root mean squared prediction error.

stress that the enteric coating of the other currently available MPA formulation (enteric-coated mycophenolate sodium) results in importantly different pharmacokinetics and that the developed LSSs only apply to the MMF formulation.[30,31]

Little is known about the pharmacokinetics of MPA in patients with AID. Comparison with pharmacokinetics in renal transplant recipients may be complicated. Most renal transplant patients are cotreated with a calcineurin inhibitor, like ciclosporin or tacrolimus. Cotreatment with ciclosporin results in a decreased EHC, due to inhibition of multidrug resistance-associated protein-2 (MRP2).[32] Furthermore, a decrease in MPA clearance over time is seen in renal transplant recipients, due to changes in renal function and albumin levels.[33,34] The results of the population pharmacokinetic model of the current study may be compared with studies describing MPA pharmacokinetics for patients in a stable posttransplantation phase receiving a ciclosporin-free regimen and including an EHC. MPA clearance in patients with AID (8.3 L/h) was slightly lower compared with renal transplant recipients cotreated with tacrolimus[24] (11.9 L/h) and healthy volunteers[35] (10.2 L/h).

In renal transplant recipients cotreated with ciclosporin, van Hest et al[36] reported a negative correlation between CrCL and MPA CL. The authors stated that MPAG CL was reduced by an impaired renal function. The increased MPA CL could be caused by displacement of MPA from albumin due to accumulation of the metabolite MPAG.[36] The covariate analysis of the current study also identified a relationship between CrCL and MPA CL. However, the correlation is positive instead of negative, MPA CL decreased with impaired renal function (Fig. 3). One reason for this different correlation is the fact that patients in this study did not use ciclosporin, which is known to inhibit EHC. Furthermore, this might be caused by an increased EHC. Decreased renal clearance of

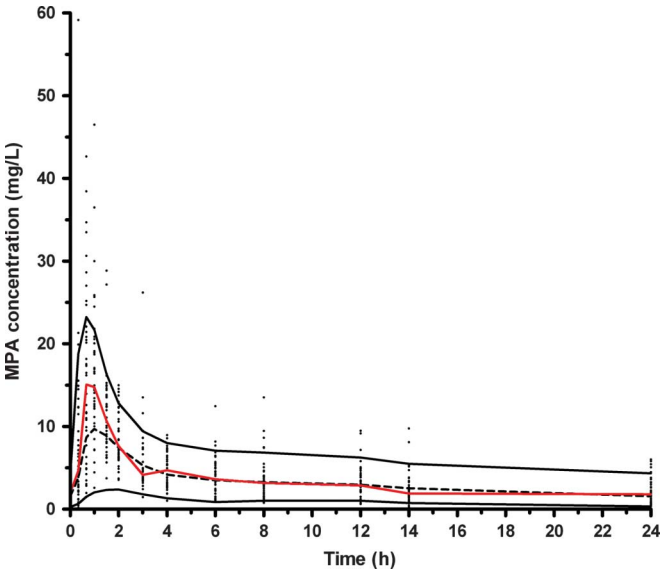

FIGURE 5. Visual predictive check. Comparison of median (dashed line) and 95- percentile interval (solid black lines) of 100 simulated data sets and observed MPA concentrations (dots). The red line represents the median observed concentration–time curve.

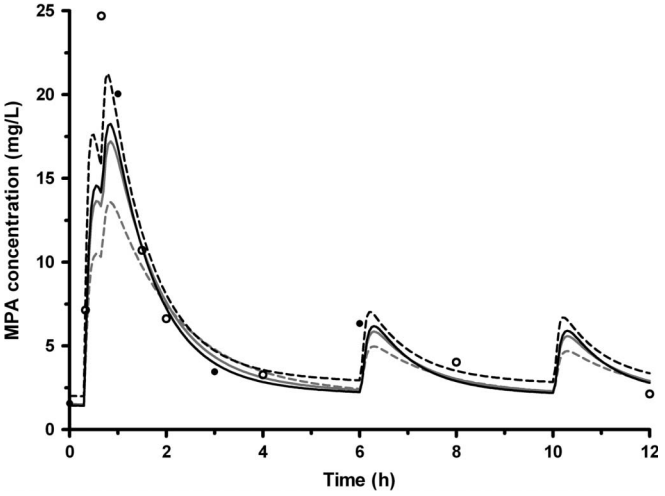

FIGURE 6. MAP-BE of the MPA concentration–time profile. The curves represent MAP Bayesian-predicted MPA concentration–time profile of a patient using 1 ($t = 0$, dashed gray line), 2 ($t = 0 + 1$, solid gray line), 3 ($t = 0 + 1 + 3$, solid black line), or 4 samples ($t = 0 + 1 + 3 + 6$, dashed black line). The filled dots represent the concentration–time points implemented in at least one of the LSSs, and the open dots represent the other observed MPA samples.

MPAG will cause accumulation of this metabolite, resulting in an increased availability of MPAG for biliary excretion. As a result, more MPAG will undergo deglucuronidation to MPA in the gut, which is reabsorbed. This explanation is supported by previous studies[37,38] in which a similar correlation was found in patients cotreated with tacrolimus.

The final model was used to develop and validate an MAP-BE to estimate $AUC_{0–12}$ on the basis of 3 sampling times within 4 hours post dose. The best LSS was based on MPA concentrations at predose, 1 and 3 hours after oral intake of MMF. Given a 10-fold IPV, and a therapeutic window from 30 to 60 $mg \cdot h^{-1} \cdot L^{-1}$ in renal transplant patients,[39] a precision of ≤25% and a bias not significantly different from zero were considered to be acceptable. The mean bias (and 95% confidence interval) of the developed LSS was −5.5% (−16.6% to 5.6%) and mean precision 23.0%, which indicates that the developed LSS has an acceptable predictive performance. Inclusion of a fourth sample during EHC (t = 6 hours) resulted in a further improvement of precision (18.9% versus 23.0%) but impairs practical application. Several MAP-BEs have been developed in renal transplant patients treated with MMF and ciclosporin.[40,41] Correlation coefficients (r^2 > 0.85) and precision (<13%) for these models are better than the values in the present study. The mean bias of a previously published MAP-BE for MPA in renal transplant patients (7.7%)[40] is comparable with the bias found in the current study (−5.5%). The better correlation coefficient and precision could be explained by the decrease in variability in the second part of the concentration–time profile, due to the inhibition of EHC by ciclosporin.[32]

For the multiple linear regression method, $AUC_{0–12}$ was best predicted when 3 samples were taken at predose and 1 and 3 hours post dose. The mean bias was less compared with the MAP-BE (0.8% versus −5.5%), but both were not significantly different from zero. The precision was comparable between both methods (22.6% versus 23.0%). Inclusion of an extra sampling time during EHC (t = 6 hours) again improved the predictive performance of the LSS slightly (precision: 17.3% versus 22.6%). Pawinski et al[9] developed an LSS for MPA with multiple linear regression in renal transplant recipients cotreated with tacrolimus with a correlation coefficient of r^2 = 0.86, which is higher compared with the current study. This might be explained by a less variability in the pharmacokinetic profile in that group of patients. Furthermore, an extension of the study using more patients may increase the correlation coefficient.

MPA concentrations in this study are determined using EMIT. A comparison of Liquid chromatography-tandem mass spectrometry and EMIT showed that EMIT overestimated MPA levels and AUC, with variations depending on the posttransplantation period and sampling time.[42] This overestimation could largely be explained by the cross-reactivity of the anti-MPA antibody with the acyl glucuronide metabolite of MPA.[43] Consequently, the LSSs developed using concentrations measured with this method cannot be used to estimate $AUC_{0–12}$ using MPA concentrations determined with other analytical methods.

In a previous study, Zahr et al[44] developed an MAP-BE using an empiric pharmacokinetic model for MMF in 20 patients with SLE. In this study, a 1-compartment model with first-order elimination convoluted with a triple γ distribution was used to fit the MPA concentration–time data. In the current study, a more mechanistic approach was used. A gallbladder compartment was connected to a 2-compartment model (Fig. 2). This extra compartment makes true circulation of MPA possible. Zahr et al[44] estimated $AUC_{0–12}$ with samples taken at 0.67, 2, and 3 hours post dose. However, predicted performance was not assessed in an independent group of patients. As a result, a comparison between the empiric method of Zahr et al and our method is not possible.

In conclusion, MAP-BEs were developed for the estimation of MPA $AUC_{0–12}$ in patients with AID taking MMF. The predictive performance of the MAP-BEs was good and comparable to those of the multiple linear regression method. Due to its flexibility with respect to sample times, the MAP-BE may be preferred over the multiple linear regression method. Optimal sampling times are predose and 1 and 3 hours after MMF administration. These results can be used for designing prospective trials, with either an observational or an interventional approach, in patients with AID, to further study the pharmacokinetic behavior of MPA and/or to study the added value of TDM for MPA in these patients.

REFERENCES

1. Knoll G. Trends in kidney transplantation over the past decade. *Drugs*. 2008;68(Suppl 1):3–10.
2. Allison AC, Eugui EM. Purine metabolism and immunosuppressive effects of mycophenolate mofetil (MMF). *Clin Transplant*. 1996;10:77–84.
3. de Winter BC, Mathot RA, van Hest RM, et al. Therapeutic drug monitoring of mycophenolic acid: does it improve patient outcome? *Expert Opin Drug Metab Toxicol*. 2007;3:251–261.
4. van Gelder T, Meur YL, Shaw LM, et al. Therapeutic drug monitoring of mycophenolate mofetil in transplantation. *Ther Drug Monit*. 2006;28: 145–154.
5. van Gelder T, Hilbrands LB, Vanrenterghem Y, et al. A randomized double-blind, multicenter plasma concentration controlled study of the safety and efficacy of oral mycophenolate mofetil for the prevention of acute rejection after kidney transplantation. *Transplantation*. 1999;68: 261–266.
6. van Gelder T, Shaw LM. The rationale for and limitations of therapeutic drug monitoring for mycophenolate mofetil in transplantation. *Transplantation*. 2005;80:S244–S253.
7. van Gelder T. Mycophenolate mofetil: how to further improve using an already successful drug? *Am J Transplant*. 2005;5:199–200.
8. Le Meur Y, Buchler M, Thierry A, et al. Individualized mycophenolate mofetil dosing based on drug exposure significantly improves patient outcomes after renal transplantation. *Am J Transplant*. 2007;7:2496–2503.
9. Pawinski T, Hale M, Korecka M, et al. Limited sampling strategy for the estimation of mycophenolic acid area under the curve in adult renal transplant patients treated with concomitant tacrolimus. *Clin Chem*. 2002; 48:1497–1504.
10. Willis C, Taylor PJ, Salm P, et al. Evaluation of limited sampling strategies for estimation of 12-hour mycophenolic acid area under the plasma concentration-time curve in adult renal transplant patients. *Ther Drug Monit*. 2000;22:549–554.
11. Le Guellec C, Buchler M, Giraudeau B, et al. Simultaneous estimation of cyclosporin and mycophenolic acid areas under the curve in stable renal transplant patients using a limited sampling strategy. *Eur J Clin Pharmacol*. 2002;57:805–811.
12. Appel GB, Radhakrishnan J, Ginzler EM. Use of mycophenolate mofetil in autoimmune and renal diseases. *Transplantation*. 2005;80:S265–S271.
13. Stassen PM, Cohen Tervaert JW, Stegeman CA. Induction of remission in active ANCA-associated vasculitis with mycophenolate mofetil in patients who cannot be treated with cyclophosphamide. *Ann Rheum Dis*. 2007;66: 798–802.

14. Glicklich D, Acharya A. Mycophenolate mofetil therapy for lupus nephritis refractory to intravenous cyclophosphamide. *Am J Kidney Dis*. 1998;32:318–322.
15. Dooley MA, Cosio FG, Nachman PH, et al. Mycophenolate mofetil therapy in lupus nephritis: clinical observations. *J Am Soc Nephrol*. 1999; 10:833–839.
16. Kapitsinou PP, Boletis JN, Skopouli FN, et al. Lupus nephritis: treatment with mycophenolate mofetil. *Rheumatology (Oxford)*. 2004;43:377–380.
17. Chan TM, Li FK, Tang CS, et al. Efficacy of mycophenolate mofetil in patients with diffuse proliferative lupus nephritis. Hong Kong-Guangzhou Nephrology Study Group. *N Engl J Med*. 2000;343:1156–1162.
18. Contreras G, Pardo V, Leclercq B, et al. Sequential therapies for proliferative lupus nephritis. *N Engl J Med*. 2004;350:971–980.
19. Sinclair A, Appel G, Dooley MA, et al. Mycophenolate mofetil as induction and maintenance therapy for lupus nephritis: rationale and protocol for the randomized, controlled Aspreva Lupus Management Study (ALMS). *Lupus*. 2007;16:972–980.
20. Neumann I, Haidinger M, Jager H, et al. Pharmacokinetics of mycophenolate mofetil in patients with autoimmune diseases compared renal transplant recipients. *J Am Soc Nephrol*. 2003;14:721–727.
21. de Winter BC, van Gelder T. Therapeutic drug monitoring for mycophenolic acid in patients with autoimmune diseases. *Nephrol Dial Transplant*. 2008;23:3386–3388.
22. Neumann I, Fuhrmann H, Fang IF, et al. Association between mycophenolic acid 12-h trough levels and clinical endpoints in patients with autoimmune disease on mycophenolate mofetil. *Nephrol Dial Transplant*. 2008;23:3514–3520.
23. Jiao Z, Ding JJ, Shen J, et al. Population pharmacokinetic modelling for enterohepatic circulation of mycophenolic acid in healthy Chinese and the influence of polymorphisms in UGT1A9. *Br J Clin Pharmacol*. 2008;65: 893–907.
24. Cremers S, Schoemaker R, Scholten E, et al. Characterizing the role of enterohepatic recycling in the interactions between mycophenolate mofetil and calcineurin inhibitors in renal transplant patients by pharmacokinetic modelling. *Br J Clin Pharmacol*. 2005;60:249–256.
25. Jonsson EN, Karlsson MO. Xpose—an S-PLUS based population pharmacokinetic/pharmacodynamic model building aid for NONMEM. *Comput Methods Programs Biomed*. 1999;58:51–64.
26. Ette EI, Williams PJ, Kim YH, et al. Model appropriateness and population pharmacokinetic modeling. *J Clin Pharmacol*. 2003;43:610–623.
27. Jadhav PR, Gobburu JV. A new equivalence based metric for predictive check to qualify mixed-effects models. *AAPS J*. 2005;7:E523–E531.
28. Shaw LM, Korecka M, Venkataramanan R, et al. Mycophenolic acid pharmacodynamics and pharmacokinetics provide a basis for rational monitoring strategies. *Am J Transplant*. 2003;3:534–542.
29. Bullingham RE, Nicholls AJ, Kamm BR. Clinical pharmacokinetics of mycophenolate mofetil. *Clin Pharmacokinet*. 1998;34:429–455.
30. Cattaneo D, Cortinovis M, Baldelli S, et al. Pharmacokinetics of mycophenolate sodium and comparison with the mofetil formulation in stable kidney transplant recipients. *Clin J Am Soc Nephrol*. 2007;2:1147–1155.
31. de Winter B, van Gelder T, Budde K, et al. Population pharmacokinetics of MPA: a comparison between EC-MPS and MMF in renal transplant recipients. *Clin Pharmacokinet*. 2008;47:827–838.
32. Hesselink DA, van Hest RM, Mathot RA, et al. Cyclosporine interacts with mycophenolic acid by inhibiting the multidrug resistance-associated protein 2. *Am J Transplant*. 2005;5:987–994.
33. Shaw LM, Mick R, Nowak I, et al. Pharmacokinetics of mycophenolic acid in renal transplant patients with delayed graft function. *J Clin Pharmacol*. 1998;38:268–275.
34. van Hest R, van Gelder T, Bouw R, et al. Time-dependent clearance of mycophenolic acid in renal transplant recipients. *Br J Clin Pharmacol*. 2007;63:741–752.
35. Jiao Z, Zhong JY, Zhang M, et al. Total and free mycophenolic acid and its 7-O-glucuronide metabolite in Chinese adult renal transplant patients: pharmacokinetics and application of limited sampling strategies. *Eur J Clin Pharmacol*. 2007;63:27–37.
36. van Hest RM, Mathot RA, Pescovitz MD, et al. Explaining variability in mycophenolic acid exposure to optimize mycophenolate mofetil dosing: a population pharmacokinetic meta-analysis of mycophenolic acid in renal transplant recipients. *J Am Soc Nephrol*. 2006;17: 871–880.
37. Naesens M, de Loor H, Vanrenterghem Y, et al. The impact of renal allograft function on exposure and elimination of mycophenolic acid (MPA) and its metabolite MPA 7-O-glucuronide. *Transplantation*. 2007; 84:362–373.
38. Borrows R, Chusney G, James A, et al. Determinants of mycophenolic acid levels after renal transplantation. *Ther Drug Monit*. 2005;27: 442–450.
39. Shaw LM, Holt DW, Oellerich M, et al. Current issues in therapeutic drug monitoring of mycophenolic acid: report of a roundtable discussion. *Ther Drug Monit*. 2001;23:305–315.
40. Le Guellec C, Bourgoin H, Buchler M, et al. Population pharmacokinetics and Bayesian estimation of mycophenolic acid concentrations in stable renal transplant patients. *Clin Pharmacokinet*. 2004;43:253–266.
41. Premaud A, Le Meur Y, Debord J, et al. Maximum a posteriori Bayesian estimation of mycophenolic acid pharmacokinetics in renal transplant recipients at different postgrafting periods. *Ther Drug Monit*. 2005;27: 354–361.
42. Premaud A, Rousseau A, Le Meur Y, et al. Comparison of liquid chromatography-tandem mass spectrometry with a commercial enzyme-multiplied immunoassay for the determination of plasma MPA in renal transplant recipients and consequences for therapeutic drug monitoring. *Ther Drug Monit*. 2004;26:609–619.
43. Schutz E, Shipkova M, Armstrong VW, et al. Therapeutic drug monitoring of mycophenolic acid: comparison of HPLC and immunoassay reveals new MPA metabolites. *Transplant Proc*. 1998;30:1185–1187.
44. Zahr N, Amoura Z, Debord J, et al. Pharmacokinetic study of mycophenolate mofetil in patients with systemic lupus erythematosus and design of bayesian estimator using limited sampling strategies. *Clin Pharmacokinet*. 2008;47:277–284.

